Parametric Optimization of Surface Roughness of Ni-W-P Electroless Coating Using Central Composite Design Coupled with Fuzzy Logic Approach

Sameer Lamichaney*, Rupam Mandal, Subhashish Sarkar, Rajat S. Sen, Buddhadeb Oraon and Gautam Majumdar

Department of Mechanical Engineering, Jadavpur University, Jadavpur, Kolkata, West Bengal, India
Corresponding author: sameer.ccct@gmail.com

Abstract

The present work studied SR of electroless Ni-W-P ternary alloy coatings on a Cu substrate. There is very little specific research conducted on the importance of reducing materials SR through Ni-W-P electroless coating, which further improves their mechanical properties. In this study, it was attempted to reduce the as-coated Ni-W-P Cu substrate surface SR by adopting DoE and optimizing the process parameters using CCD. The aim was to optimize the desired response controlled by multiple input parameters. ANOVA and regression analysis were implemented to indicate the significance of as-coated substrates parameters and their impact on the measured SR responses. From CCD optimization, optimal SR parameters were found to occur at low values. Furthermore, FL approach was employed to predict Ni-W-P electroless coating SR, as compared to experimental and CCD approaches. It was found that fuzzy measured values were in good agreement with experimental and CCD values. There was a small difference among all values, and response optimization predicted optimal conditions comparatively well. Therefore, the developed models can be effectively used to predict SR. Moreover, confirmation tests were performed to validate that CCD optimized levels and developed fuzzy models effectively represented SR. Optimized parameters characterization was done with the help of SEM and EDX. It was seen that globular shaped atoms were scattered all over the sample, while granular grains were more clear. From EDX, appropriate deposition of Ni-W-P substrate in Cu was found. Thus, it was concluded that Ni-W-P incorporation in the Cu substrate made a major contribution to the film morphology, enhancing the metal properties and reducing SR.

Keywords: CCD; contour plot; Cu substrate; EDX; electroless coating; FL; MF; microstructure; Ni-W-P coatings; SEM; SR.

Introduction•

Surface quality is an essential requirement in mechanical engineering due to its impact on product performance. Surfaces characteristics highly influence materials ability to withstand stress, temperature, friction and corrosion [1].

• The abbreviations list is on page 192.

SR plays an important role for the tribological operation of any component. SR characteristics are: center line R_a; root mean square roughness- R_q; skewness- R_{sk}; kurtosis- R_{ku}; and mean line peak spacing- R_{sm} [2].

In order to reduce SR and enhance materials mechanical properties, the present study researched electroless coating using CCD. Electroless coating is a chemical reduction process in which chemical composition is used for metals deposition without the use of electricity [3]. The main goal of this deposition process is to increase corrosion, wear and abrasion resistance by reducing SR of the Cu substrate material.

Among all coatings, Ni–P is the most common type of electroless coating [4]. In order to further improve the properties of electroless Ni-P coatings, several ternary Ni-X–P coatings have been developed, where X is typically a transition metal such as W, Co, Mn, Mo, Cu and Re.

The present study focused on W alloy in electroless Ni-P coating, because it exhibits unique properties such as high melting point and hardness [5-6]. It was seen that about 3.8 wt.% W was co-deposited with Ni, which caused a reduction in P content of the deposit from 8.9 to 2.3 wt.%, and resulted in a crystalline structure of the film [7]. It was confirmed that W co-deposition in a Ni-P matrix reduces P content of the deposit and alters the crystal structure, according to [7-8]. Herein, SR measurements were taken before and after coating deposition. Specimens with almost equivalent SR values were used in wear and friction tests. Measurements were taken using Talysurf profilometer (Surtronic 3$^+$, Taylor Hobson) [9-10], which was is equipped with a diamond stylus having a tip radius of 5 μm, and used 0.8 and 4 mm traversing and sampling lengths, respectively.

SR measurements on the coated samples were repeated at least four times and an average of four values were recorded. The results showed that SR and friction coefficient were dependent of the Ct of W in the film. It is possible that an increase in the Ct of W may promote a decrease in SR. The smoothest surfaces yielded friction coefficient lowest values in as-deposited coatings. A nodular structure, with a cauliflower shape, is often associated with a reduced friction coefficient [11-12].

At lower Ct of the surfactant, the surface finish was poor, but it significantly improved when the Ct exceeded 0.6 g/L. [13-14]. It was found that the nodular nature of the electroless coatings shown by SEM was responsible for a surface profile rougher than sputtered coatings [15].

Optimization of the process parameters is the major challenge in experimental work to save labor, materials and money, as well as to obtain an improved response. So, the latest and advanced statistical tools must be adopted within the investigation boundary conditions.

RSM is a highly advanced DoE technique, which includes statistical formulation for developing a model and analyzing a process which aims to optimize the desired response controlled by multiple input parameters [16-17]. Employing a relatively small number of experiments, RSM can be used to map a design space. CCD method alone is satisfactory enough for handling single goal problems, but not acceptable to deal with multi objective issues. These multi objective challenges are normally solved by assigning individual weights to the responses according to

priority. In all, these theories are assigned based on assumptions, which may lead to uncertainty in results [18-20].

In this study, FL approach was used to overcome all these assumptions, and to clear up any doubts. It is a method that gives values for areas where there are no clear borderlines among variables, and which supports the decision-making process. This theory was introduced by [21], in 1965. FL is widely employed to build inference systems that support decisions making and management of the manufacturing system [22]. It is a mathematical theory of inexact reasoning which allows modelling of human intellectual processes in linguistic terms [23]. FL is based on intuition and judgment, and it does not need a mathematical model to construct theories [24].

The existing research in Ni-W-P electroless coating has primarily focused on optimizing the deposition process and exploring materials properties. However, a significant research gap exists in comprehensively addressing the SR of coated substrates. Limited attention has been given to systematic investigation and optimization of the parameters affecting SR in Ni-W-P electroless coatings. This gap hinders the knowledge of how to effectively reduce SR, which is crucial for enhancing functional and mechanical properties of coated materials.

The aim of this research was to optimize the parameters of Ni-W-P electroless coatings for reducing SR of the Cu substrate. This optimization was achieved by employing both CCD and FL approaches, with a subsequent comparison of the results, to attain the lowest SR. The coating elements that underwent the optimization process included $Na_2WO_4.2H_2O$, $NaH_2PO_2.H_2O$ and $NiSO_4.6H_2O$.

Experimental details

Cu sheets (Cu with 99% purity, procured from Lobochemie Pvt ltd.) with the dimensions $20 \times 15 \times 0.1$ mm were used as substrates for the deposition of electroless Ni–W–P coatings. The prepared Cu samples were exposed to surface pre-treatment before immersion in the electroless bath samples, to remove the oxide layer and carbonized hydrocarbon formation. For this purpose, the samples were rinsed with distilled water for 2 min, and then cleaned with 25% diluted HCl, for 10 min, at room temperature. Activation is also a very important step of samples preparation. Herein, the specimens were activated with a $PdCl_2$ solution, for 8-10 s, at 55 °C, followed by rinsing with distilled water, for a few seconds. After surface activation, the samples were immersed in the Ni-W-P electroless bath. The electroless bath composition is shown in Table 1.

Table 1: Composition of Ni-W-P bath.

Bath composition	Quantity
$Na_2WO_4.2H_2O$	15-20 gm/L
$NaH_2PO_2.H_2O$	25-35 gm/L
$NiSO_4.6H_2O$	35-45 gm/L
$Na_3C_6H_5O_7.2H_2O$	32 gm/L
$CH_3COONa.3H_2O$	4 gm/L
pH value	5.9
Time	1 h
Bath volume	200 cm^3
Temperature	85 °C

CCD

CCD is an effective tool of DoE which evaluates the individual effect of each process parameter on the responses, by conducting a minimum number of experiments [8]. S/N ratio finds the best level of each parameter for a particular response based on qualitative characteristics such as lower the better, higher the better and nominal the better [9]. Irrespective of the chosen qualitative characteristics for a particular response, the levels with higher S/N ratios for the corresponding factors are deemed to be optimal for that particular response. Contour and surface graphs are often used to explain both linear and nonlinear mixing complexities of mixed components. In RSM technique, CCD: offers more understanding than that of the three factorial designs; and it needs less experimental runs, despite showing significant optimization for most stable processes. CCD is the most widely used RSM and includes a factorial or factorial fractional design with center points, supported by a group of axial points [27].

The experiment was based on CCD to study the combined effects of three independent variables: $Na_2WO_4.2H_2O$, $NaH_2PO_2.2H_2O$ and $NiSO_4.6H_2O$. A total of 20 runs, 3 factors and 3 levels of factorial CCD were used to optimize the SR of Ni-W-P electroless coating using Design Expert Software. To establish the importance of individual process parameters and their interactions, a regression equation was formulated, which estimates the correlation between responses and input process parameters.

S/N ratio is a valuable tool in experimental design, to assess and optimize the relationship between input parameters and response variables based on qualitative characteristics. The specific calculation of S/N ratio formula will vary depending on the qualitative characteristic, and whether ones wishes to minimize, maximize or reach a target value for a given response variable.

S/N ratio is calculated based on specific qualitative characteristics associated with the response variable. These characteristics depend on the response nature. There are typically three categories: lower the better- in situations where the goal is want to minimize the response (e.g., SR), where a lower S/N ratio indicates a better outcome; higher the better- conversely, in cases where the aim is to maximize the response (e.g., yield or tensile strength), where a higher S/N ratio indicates a better outcome; and nominal the better- in some cases, the objective may be to obtain response that is close to a target value, neither too far nor too near. Herein, lower the better S/N ratio was preferred, if it was closer to the target value.

FL interference system

FL is an artificial intelligence technique which has proved to be a very useful tool for modelling and analysing complex inter-relationships between process parameters and response variables [18]. Fuzzy modelling is comprised of three steps that include fuzzification, rule framing and defuzzification processes. In the first stage, fuzzification process is done. With the help of connection description, each factor and a well-defined numeric value are preserved [23-24]. In the second stage, rules are considered by the combination of parameters using logical operators. Finally, defuzzification is done in which all connection degrees are turned into a quantifiable value by combining outputs of the framed rules [25-26]. Variables, i.e.,

$Na_2WO_4.2H_2O$, $NaH_2PO_2.H_2O$ and $NiSO_4.6H_2O$, are taken as inputs in the fuzzy inference system, where SR is considered as output (Fig. 1). A fuzzy-based rule is defined, which predicts SR in the fuzzy domain, and the fuzzy interference engine is considered as "Mamdani". Mamdani shows relatively better results [27]. Therefore, in modelling the algorithm, the system outputs are calculated based on the centroid method, and Mamdani implication is used for defuzzification [28-29].
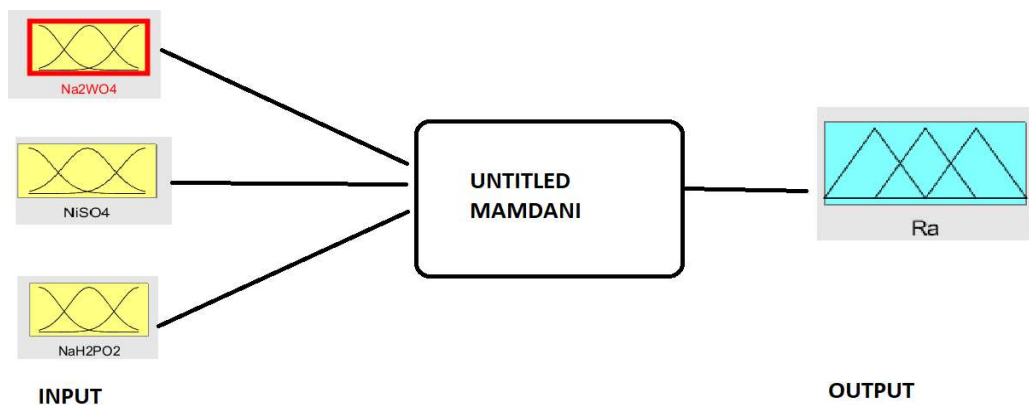
Figure 1: Three input and single output fuzzy interference system.

Results and discussion

The roughness measurements are quoted in terms of SR values. SR values refer to parameters that characterize R_a. R_a value is defined as the arithmetic mean of the absolute values of the distances from the mean line of the valleys and the peaks [13]. There were total 20 runs that were conducted in the CCD design. Based on the different parameters, R_a reading was calculated with the help of Talysurf profilometer. R_a experimental results for different sets of experiments as coded forms are given in Table 2.

Table 2: Results of coded values with R_a.

Run number	Factor 1, X1 $Na_2WO_4.2H_2O$	Factor 2, X2 $NaH_2PO_2 2H_2O$	Factor 3, X3 $NiSO_4.6H_2O$	R_a (µm)
1	15	25	45	0.635
2	13.2955	30	40	0.891
3	17.5	30	40	0.572
4	17.5	38.409	40	0.553
5	17.5	30	40	0.598
6	20	25	45	0.806
7	17.5	21.591	40	0.831
8	17.5	30	48.409	0.858
9	20	25	35	0.868
10	17.5	30	40	0.521
11	21.7045	30	49	0.667
12	17.5	30	40	0.519
13	17.5	30	31.591	0.661
14	20	35	35	0.664
15	20	35	45	0.71
16	15	25	35	0.837
17	15	35	35	0.732
18	17.5	30	40	0.525
19	17.5	30	40	0.546
20	15	35	45	0.907

The final CCD obtained for R_a with significant terms was quadratic in actual and coded equation. To evaluate the relationship between response and variables, the following regression equation for deposited R_a in terms of actual factors is given as follows:

Final equation in terms of actual factors

$$Surface\ roughness = +33.94 - 3.85 * x_1 - 1.72 * x_2 - 3.65 * x_3 - 0.21 * x_1 * x_2 + 0.0014 * x_1 x_3 + 0.11 * x_2 * x_3 + 0.61 * x_1^2 + 0.09 * x_2^2 + 0.14 * x_3^2 \tag{1}$$

Through this regression equation, we will be able to get the response value of each parameter.

Optimization of parameters for R_a through mathematical calculation

In order to optimize the process parameters and the response (R_a), we can use the equation 3.1. The optimum values for process parameters can be obtained by differentiating the equations w.r.t. x_1^*, x_2^* and x_3^*. The equation that we get is 3.1a, 3.1b and 3.1c given below:

$$\frac{\partial s}{\partial x_1} = 0$$

$$\text{i. e. } 1.22x_1 - 0.21x_2 + 0.0014x_3 = 3.85 \tag{2}$$

$$\frac{\partial s}{\partial x_2} = 0$$

$$\text{i. e. } -0.21x_1 + 0.18x_2 + 0.11x_3 = 1.72 \tag{3}$$

$$\frac{\partial s}{\partial x_3} = 0$$

$$\text{i. e. } -0.0014x_1 + 0.11x_2 + 0.28x_3 = 3.65 \tag{4}$$

Using equation 1, 2 and 3, one obtains the following optimum solutions of x_1^*, x_2^* and x_3^*, as given below:

$$\begin{pmatrix} 3.85 \\ 1.72 \\ 3.65 \end{pmatrix} = \begin{pmatrix} 1.22 & -0.21 & 0.0014 \\ -0.21 & 0.18 & 0.11 \\ -0.0014 & 0.11 & 0.28 \end{pmatrix} \begin{pmatrix} x1 \\ x2 \\ x3 \end{pmatrix}$$

Solving the above matrix, the optimized value for x_1^*, x_2^* and x_3^* can be considered as:

$$x_1^* = 4.759\ , x_2^* = 9.379,\quad x_3^* = 9.375 \tag{5}$$

Since the bath volume was 250 mL, when converting the value of x_1^*, x_2^* and x_3^* into gm/L, one obtains: $Na_2WO_4.2H_2O$ = 19.04 gm/L; $NaH_2PO_2 2H_2O$ = 37.52 gm/L; and $NiSO_4. 6H_2O$ = 37.52 gm/L.

Putting the value of x_1^*, x_2^* and x_3^* in equation 5, the optimum response for R_a is 0.522 µm.

ANOVA for R_a

From Table 3, F and p-value can be analysed.

Table 3: ANOVA for response R_a quadratic model.

Source	Sum of squares	DF	Mean square	F value	p-value	Prob > F
Model	0.30	9	0.034	6.17	0.0044	significant
A-X1	0.014	1	0.014	2.61	0.1374	
B-X2	0.026	1	0.026	4.86	0.0520	
C-X3	6.087E-003	1	6.087E-003	1.12	0.3146	
AB	0.027	1	0.027	5.02	0.0490	
AC	1.513E-005	1	1.513E-005	2.785E-003	0.9589	
BC	0.029	1	0.029	5.41	0.0423	
A^2	0.10	1	0.10	19.23	0.0014	
B^2	0.043	1	0.043	7.85	0.0188	
C^2	0.088	1	0.088	16,24	0.0024	
Residual	0.054	10	5.430E-003			
Lack of fit	0.049	5	9.826E-003	9.50	0.0137	significant
Pure error	5.171E-003	5	1.034E-003			
Corr total	0.36	19				

Model F-value of 6.17 implies that the model is significant. There is only a 0.44% chance that a "Model F-Value" this large could occur due to noise. Model p-value of 0.0044 also implies the model is significant. P-values less than 0.0500 indicate model terms are significant.

In this case, AB, BC, A2, B2, C2 are significant model terms. Values greater than 0.1000 indicate that the model terms are not significant. Lack of fit F-value of 9.50 implies that it is significant. There is only 1.37% chance that a lack of fit F-value this large could occur due to noise.

Table 4 shows R^2 of 0.8475, which is is considered to be a significant value in order to proceed with the design for further analysis. AP measures S/N ratio. A ratio greater than 4 is desirable. Herein, S/N ratio of 6.894 is adequate. This model can be used to navigate the design space. Considering the values of all ANOVA statistical parameters, the model results were found to be significant in this work.

Table 4: ANOVA results for SR.

SD	0.074
Mean	0.70
CV%	10.60
R^2	0.8475
Adjusted R^2	0.7102
Predicted	0.1093
PRESS	0.39
AP	6.615

Discussion on 3-D and contour plot for R_a

Fig. 2 shows the second-order 3D response surface plot along with the contour plot of R_a as a function of Ct of $Na_2WO_4.2H_2O$ and $NaH_2PO_2.2H_2O$, keeping $NiSO_4.6H_2O$ constant. SR plot in Fig. 2(a) indicates that it rose with an increase in the Ct of $Na_2WO_4.2H_2O$ and of $NaH_2PO_2.H_2O$. Fig. 2(b) shows SR along with contour plot as a function of Ct of $Na_2WO_4.2H_2O$ and $NaH_2PO_2.2H_2O$. This contour plot indicates that the surface was not symmetric and that peaks were not in the center.

<div align="center">

(a)   *(b)*

</div>
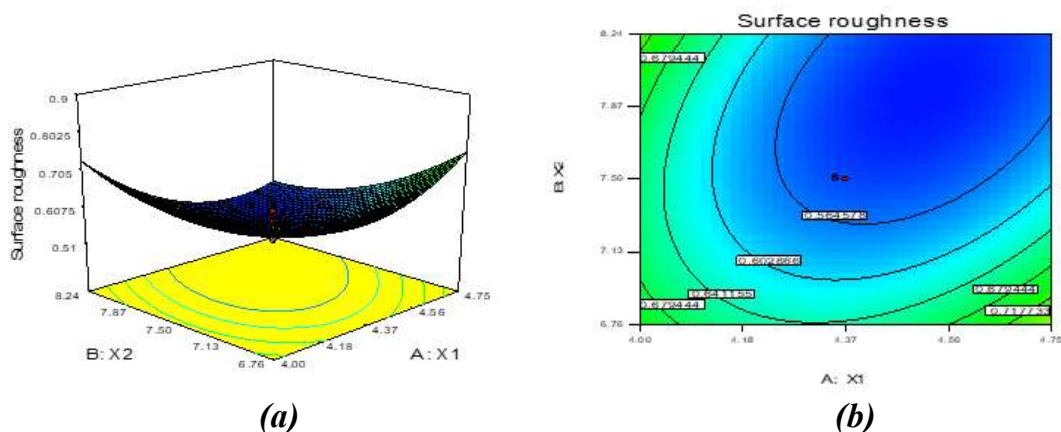
Figure 2: Second order 3-D and contour plot showing interaction effect of X1 and X2 with response to SR.

Fig. 3 shows second-order 3D response surface plot along with SR contour plot as a function of Ct of $Na_2WO_4.2H_2O$ and $NiSO_4.6H_2O$, keeping $NaH_2PO_2.2H_2O$ constant.

<div align="center">

(a)   *(b)*

</div>
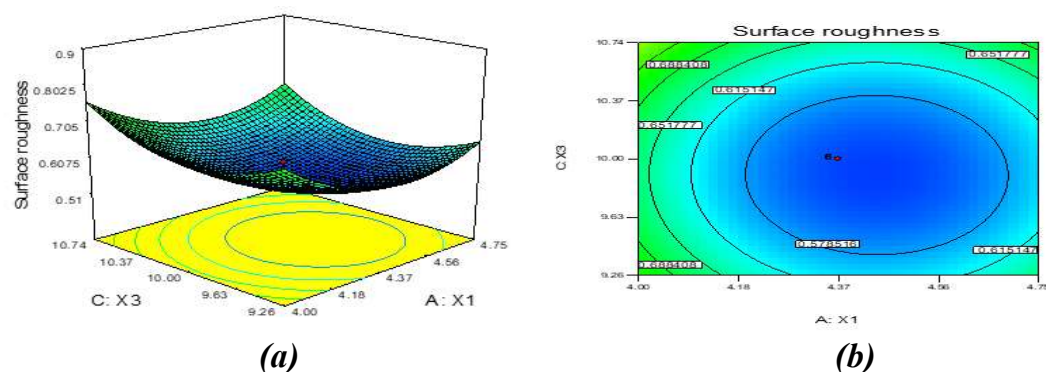
Figure 3: Second order 3-D and contour plot showing interaction effect of X1 and X3 with response to SR.

Fig. 3(a) shows that SR remained constant with Ct of $Na_2WO_4.2H_2O$, but decreased with the rise in Ct of $NiSO_4.6H_2O$. Fig. 3(b) shows that the peak surface is symmetric and that peaks are in the center. Therefore, the interaction between X1 and X3, keeping X2 constant, had significant results.

Fig. 4 shows the second-order 3D response surface plot along with the contour plot of SR, as a function of Ct of $NaH_2PO_2.2H_2O$ and $NiSO_4.6H_2O$, keeping $Na_2WO_4.2H_2O$ constant.

Figs. 2-4 show that the interaction between X1 and X3, keeping X2 constant, had a more significant response than the other two, and that SR parameters had great response.

Fig. 4(a) shows that SR decreased at high rate with Ct of $NaH_2PO_2.2H_2O$, but did not show much changes in deposition with the rise in Ct of $NiSO_4.6H_2O$. Fig. 4(b) shows that the peak surface was not symmetric and that peaks are not in the center. Interaction between X2 and X3, keeping X1 constant, did not indicate significant results.

(a)   *(b)*
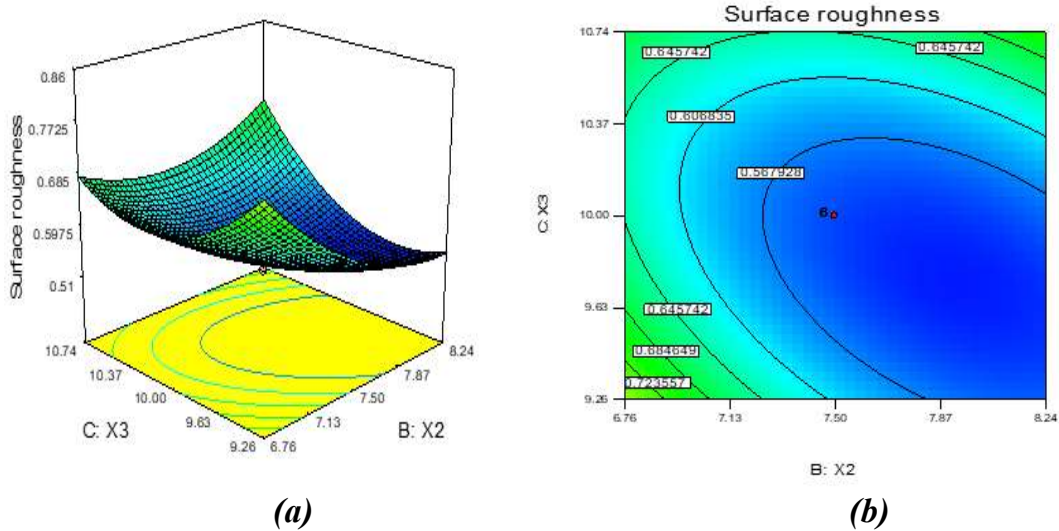
Figure 4: Second order 3-D and contour plot showing interaction effect of X2 and X3 with response to SR.

Fig. 5 shows optimized parameters: $Na_2WO_4.2H_2O$ = 18.8166 gm/L, $NaH_2PO_2.2H_2O$ = 34.8415 gm/L and $NiSO_4.6H_2O$ = 37.5368 gm/L. The optimum response for SR was 0.511 µm.
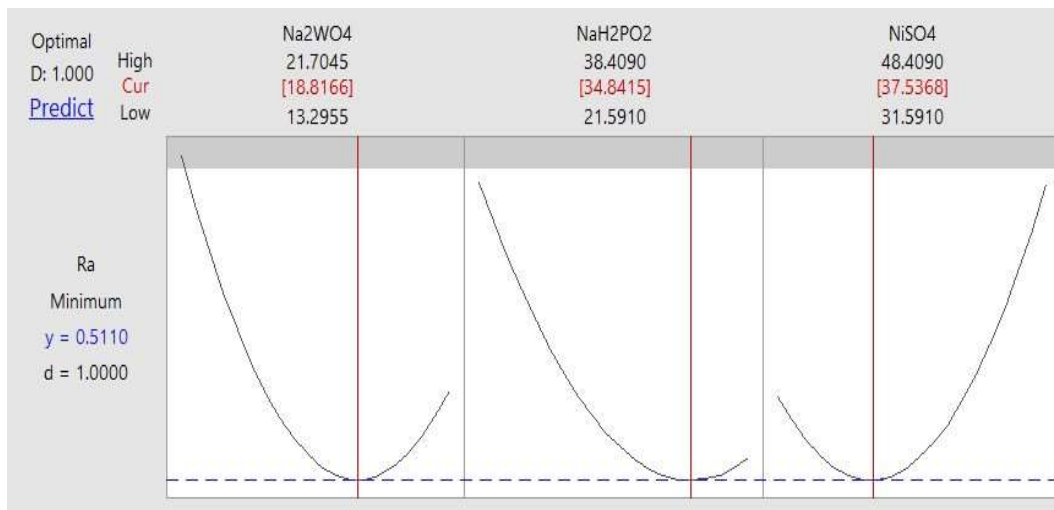
Figure 5: Optimized parameter with optimum response for SR.

Fuzzy modelling for SR

From the aforesaid CCD analysis, it is apparent that the electroless Ni-W-P ternary alloy coatings on the Cu substrate produced lower SR. Therefore, experimental data of the electroless Ni-W-P alloy coating were used for the fuzzy-based algorithm to predict SR at different process parameters. In this regard, a conceptual framework based on FL algorithm was designed in MATLAB®(R2018b) (Figs. 6-9). Triangular MF was considered in this study. In the developed algorithm, the input and output variables were fuzzified into three fuzzy sets: low (L), medium (M) and high (H). The input variables and output variables are shown in Figs. 6-9.
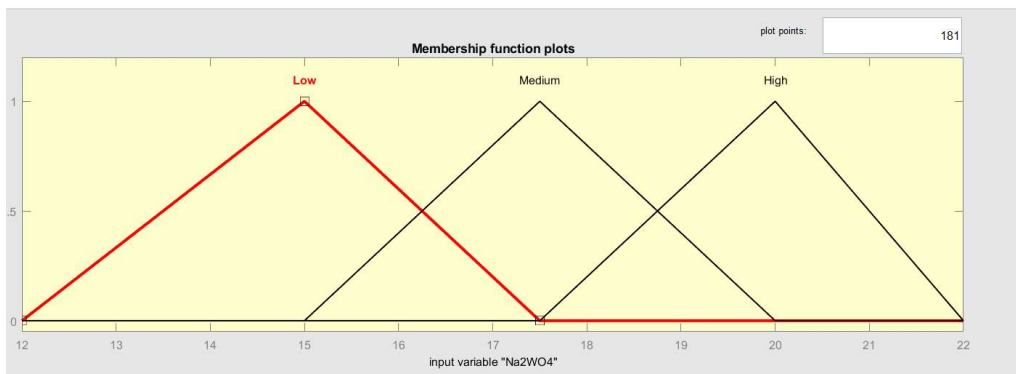
Figure 6: MF of $Na_2WO_4.2H_2O$.
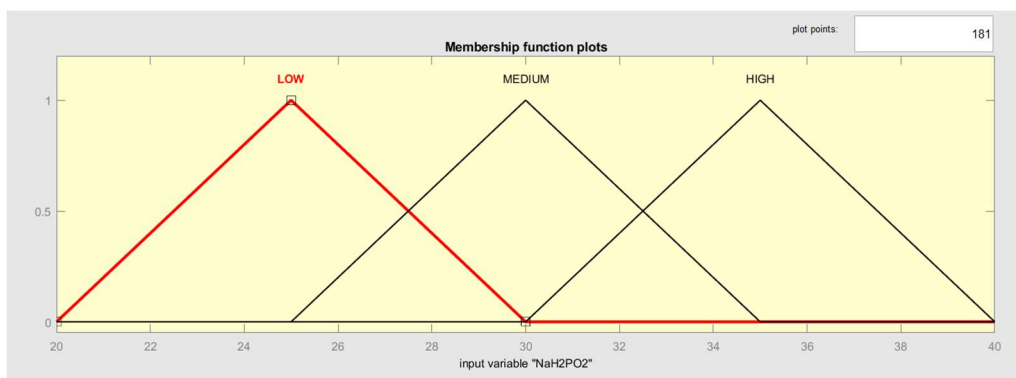
Figure 7: MF of $NaH_2PO_2.2H_2O$.
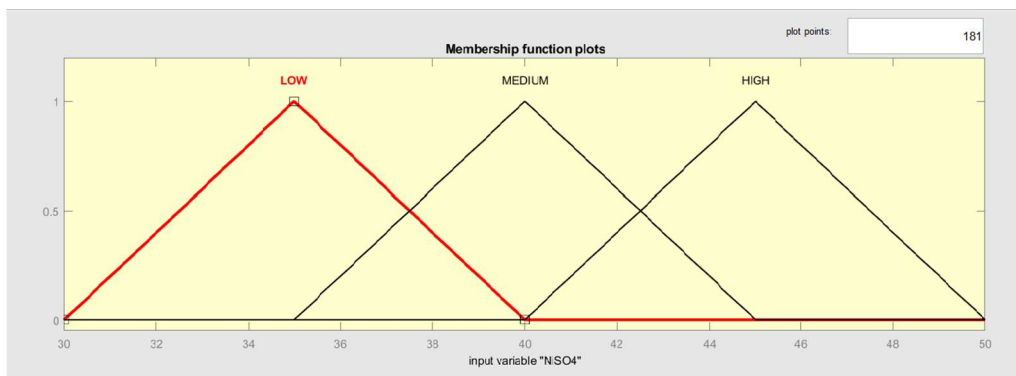
Figure 8: MF of $NiSO_4.6H_2O$.
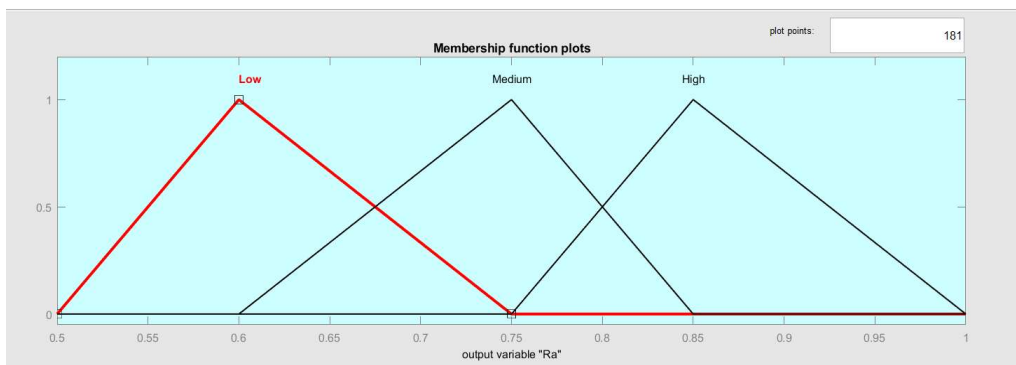
Figure 9: Output of SR variables.

The detailed parameters of fuzzy inference system with triangular MF are given in Table 5.

Table 5: Fuzzy rules expression.

Rule no.	IF			SR
	$Na_2WO_4.2H_2O$	$NaH_2PO_2.2H_2O$	$NiSO_4.6H_2O$	
1	H	L	L	H
2	L	M	M	M
3	L	H	M	L
4	H	H	M	L
5	L	M	H	L
6	H	M	M	M
7	M	M	M	L
8	H	L	H	H
9	M	M	M	L
10	M	M	H	H
11	H	H	H	M
12	M	M	M	L
13	M	M	M	L
14	L	L	H	M
15	L	L	L	H
16	M	M	L	M
17	L	H	H	H
18	M	M	M	L
19	L	H	L	H
20	M	L	M	H

Fuzzy rule SR graph

Fig. 10 shows FL graph. The yellow-coloured triangles of the input variables indicate the MF to which the input value belongs. Blue colour triangle of SR indicates the MF of output value yield from the input values of the system based on the adapted fuzzy rules. SR prediction value used the input parameters: $Na_2WO_4.2H_2O$ = 18.8 gm/L; $NaH_2PO_2.2H_2O$ = 34.8 gm/L; and $NiSO_4.6H_2O$ = 37.5 gm/L. The output SR value was 0.625 μm.
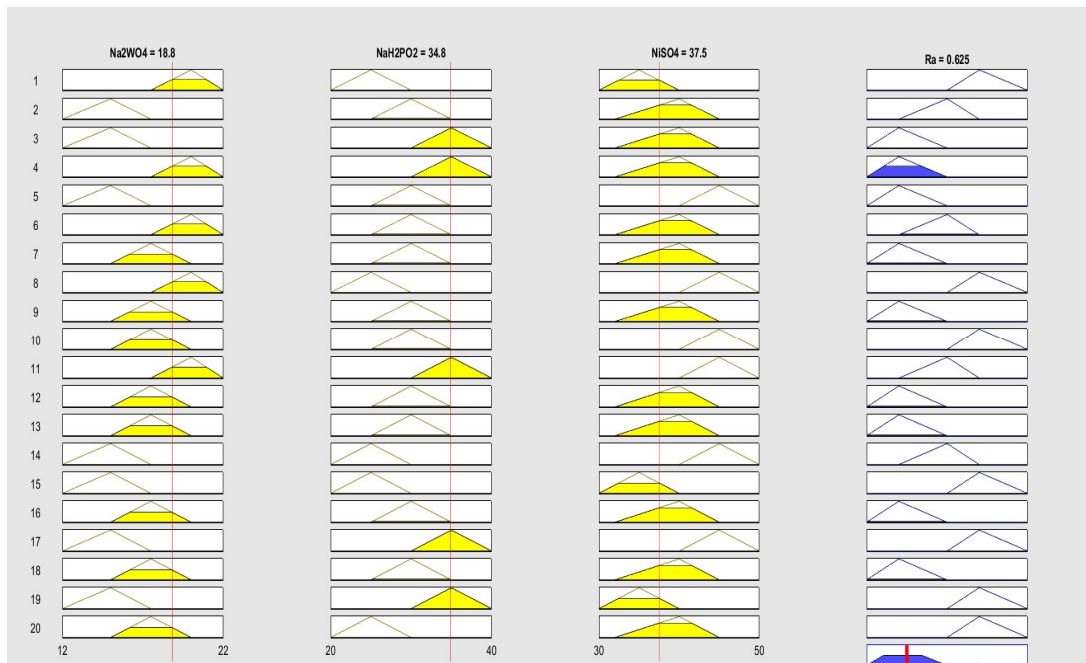
Figure 10: Fuzzy rule R_a graph.

Surface view of SR

Surface view of SR against $NaH_2PO_2.2H_2O$ and $Na_2WO_4.2H_2O$ is plotted in Fig. 11. Steep slopes of contrasting nature of SR are observed when $Na_2WO_4.2H_2O$ is higher. When $NaH_2PO_2.2H_2O$ is increased, SR decreases. A plane SR corresponding to 0.650 μm and lower was observed.
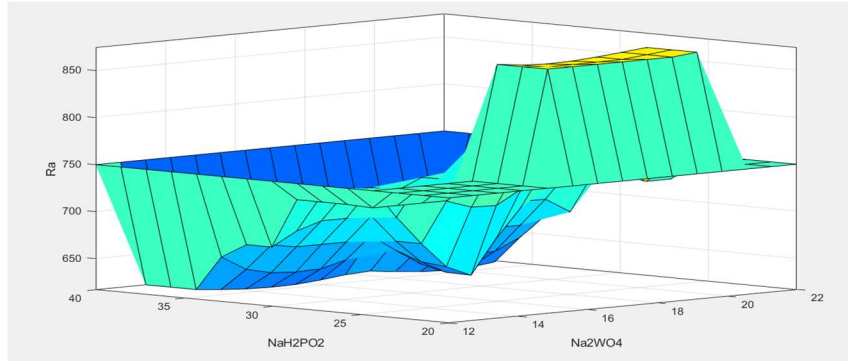
Figure 11: Surface view of SR *vs.* $NaH_2PO_2.2H_2O$ and $Na_2WO_4.2H_2O$.

Fig. 12 shows that, with an increase in $NiSO_4.6H_2O$ to 40 gm/L, SR drastically decreased. However, with an increase in $Na_2WO_4.2H_2O$, SR increased. Similarly, in Fig. 13, SR decreased when $NaH_2PO_2.2H_2O$ and $NiSO_4.6H_2O$ ranged from 25 to 30 gm/L and 35 to 40 gm/L, respectively.
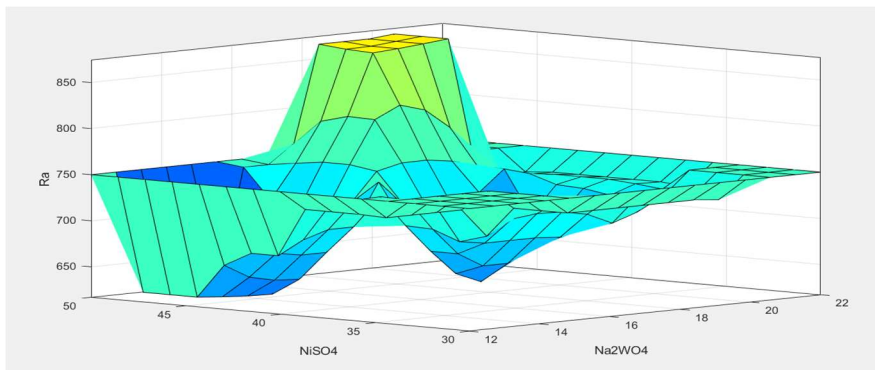
Figure 12: Surface view of SR *vs.* $NiSO_4.6H_2O$ and $Na_2WO_4.2H_2O$.
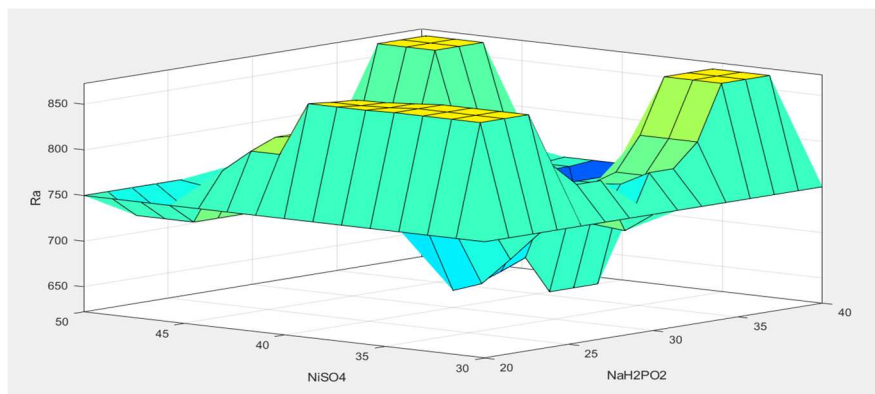
Figure 13: Surface view of SR *vs.* $NiSO_4.6H_2O$ and $NaH_2PO_2.2H_2O$.

This complements the fact that all SR parameters were correlated to each other and had a similar effect on the outcome.

Comparison and validation test

The authentication tests are an essential step for the verification of the results obtained from CCD approach [23]. Therefore, validation experiments at the optimized process parameters were conducted for SR. Mathematical results formed from CCD regression equation were compared with the predicted average based on CCD optimal process parameters and FL values. Fig. 14 shows that there is a small difference among all values. The response optimization predicted optimal conditions comparatively well.
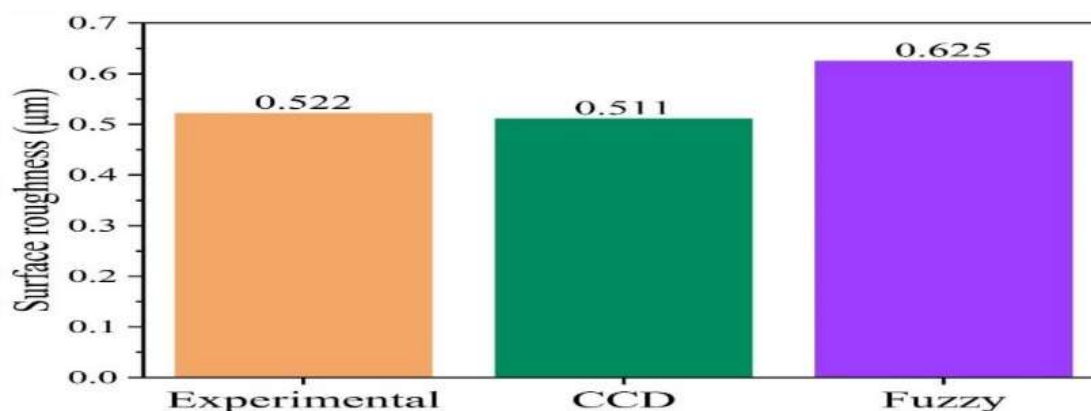
Figure 14: Comparative chart.

Study of microstructure

Under SEM micrograph, the characteristics of the electroless Ni-W-P deposit have been further analyzed. Fig. 15 is the SEM of Cu substrate without coating, which shows elongated grains of the substrate with no defined grain boundary.
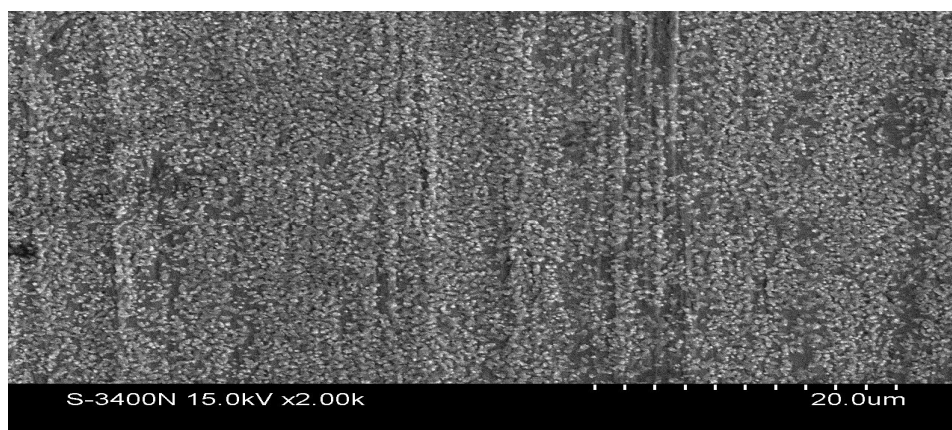
Figure 15: SEM of the Cu substrate without coating.

Fig. 16 (a) and (b) show the SEM of Cu substrate after Ni-W-P coating, at 20 and 50 µm, respectively, where the oval shape disintegration for the electroless deposit

is visible. All the samples after Ni-W-P electroless coating deposition indicate a disc type precipitate of metallic phosphide on the Cu substrate. It is seen that the globular shaped atom scattered all over the sample, and that granular grains are more clear.

| (a) | (b) |
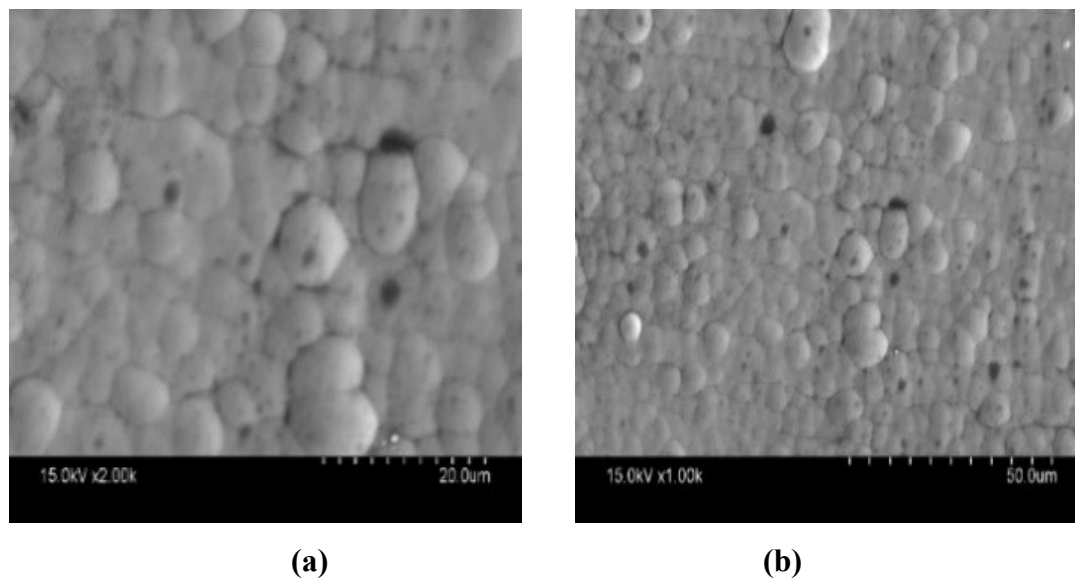
Figure 16: SEM of the Cu substrate after electroless Ni-W-P coating.

SEM analysis has provided evidence that Ni, W and P addition, in the form of a Ni-W-P coating, had a beneficial effect on the material's microstructure, leading to improvements in its properties. The specific nature of these improvements will depend on the intended application and the desired material characteristics, which may include SR reduction. So, SEM analysis indicated that Ni-W-P incorporation greatly contributed to the morphology of the film, to enhance Cu properties.

Study of composition in as-coated substrate
The percentages of Ni, P and W in the electroless Ni-W-P deposits were determined using an EDX micro-analyzer coupled to SEM (Table 6). EDX analyses of as-coated samples are shown in Fig. 17.
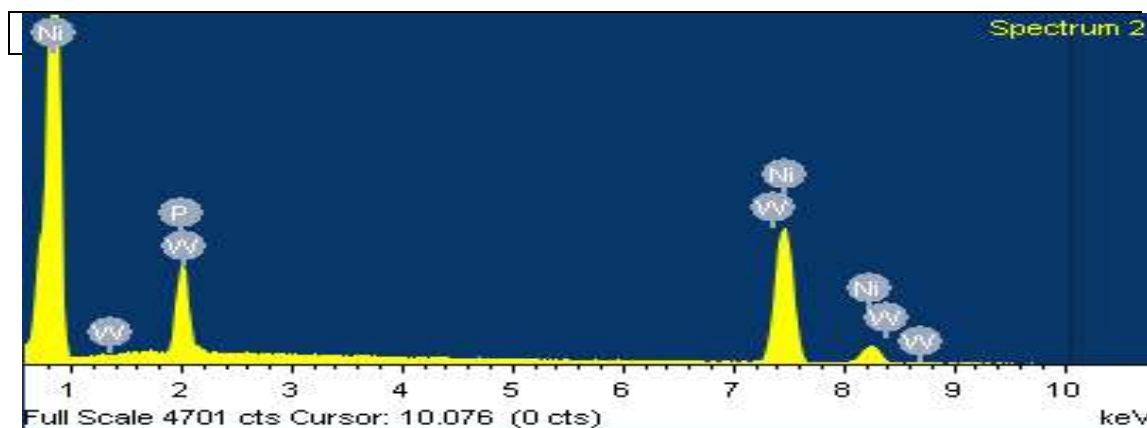
Figure 17: EDX analysis of the as-coated substrate.

Table 6: Weight percentage of elements in the as-deposited substrate.

Element	Weight%	Atomic%
$NaH_2PO.2H_2O$	8.30	14.74
$Na_3C_6H_5O_7.2H_2O$	89.69	84.96
$Na_2WO_4.2H_2O$	2.01	0.30
Totals	100.00	

Conclusions

In this study, SR parameters, like centre line R_a, were efficiently optimized using Fuzzy theory along with CCD method in Ni–W–P electroless coatings. The three parameters ($Na_2WO_4.2H_2O$, $NaH_2PO_2.2H_2O$ and $NiSO_4.6H_2O$) were fuzzified to optimize SR parameters through a single comprehensive output measure (R_a).

Optimized parameters for lower R_a which were obtained from regression predicted values through CCD model were: $Na_2WO_4.2H_2O$ = 18.8166 gm/L; $NaH_2PO_2.2H_2O$ = 34.8415 gm/ L; and $NiSO_4.6H_2O$ = 37.5368 gm/ L. The optimum response for R_a was 0.511 μm.

In terms of FL observation, it was found that R_a prediction value in input parameters was: $Na_2WO_4.2H_2O$ = 18.8 gm/L; $NaH_2PO_2.2H_2O$ = 34.8 gm/L; and $NiSO_4.6H_2O$ = 37.5 gm/L. The output R_a value was 0.625 μm.

Regression predicted and fuzzy predicted values were fairly close to experimental values i.e., $Na_2WO_4.2H_2O$ = 19.04 gm/L, $NaH_2PO_2.2H_2O$ = 37.52 gm/L and $NiSO_4.6H_2O$ = 37.5 gm/L. The optimum response for R_a was 0.522 μm. This shows that: there was a small difference among all values; and that the response optimization predicted optimal conditions comparatively well.

From the above observations, it may be concluded that the as-deposited Ni-W-P electroless coating substrate had lower SR. R_a value was 0.511 μm, whereas SR value of Cu substrate without coating was 1.19 μm. Clearly, the optimized as-deposited coated samples showed a significant decrease of 49.74% in SR compared to the substrates without coating.

SEM analysis showed that the Cu substrate without coating had elongated grains of the substrate with no defined grains boundaries, while in the as-deposited coating substrate oval shape disintegration is visible. Globular shaped atom was scattered all over the sample and grains were seen more precisely. This indicates that Ni-W-P incorporation made a major contribution to the film morphology, enhancing Cu properties. EDX showed Ct of Ni, P and W in the optimized coating. From this study, it was concluded that W content played a significant role in reducing the R_a of ternary Ni-W-P electroless coating. The proposed methodology may be taken as an effective approach for optimizing R_a parameters in industrial experiments, and helping researchers.

Authors' contributions

Sameer Lamichaney, Rupam Madal: contributed to conceptualization, design, methodology, data collection, analysis, investigation, writing (original draft), literature review and editing. **Subhasish Sarkar**: contributed to conceptual framework, discussion and conclusion. **Rajat S. Sen, Buddhadeb Oraon, Gautam Majumdar**: contributed to supervision, resources and validation.

Abbreviations
ANOVA: analysis of variance
AP: adequate precision
CCD: central composite design
CH₃COONa.3H₂O: sodium acetate
Ct: concentration
Cu: copper
CV: coefficient of variation
DoE: design of experiments
EDX: energy dispersive X-ray
FL: fuzzy logic
HCl: hydrochloric acid
MF: membership function
Na₂WO₄.2H₂O: sodium tungsten dihydrate
Na₃C₆H₅O₇.2H₂O: tri-sodium citrate dihydrate
NaH₂PO.2H₂O: sodium hypophosphite
Ni: nickel
NiSO₄.6H₂O: sodium sulphate
P: phosphorus
PdCl₂: palladium chloride
PRESS: predicted residual sum of squares
R²: coefficient of determination
Rₐ: average roughness
Re: rhenium
RSM: response surface methodology
SD: standard deviation
SEM: scanning electron microscopy
S/N: signal-to-noise ratio
SR: surface roughness
W: tungsten

References
1. Basheer C, Dabade UA, Suhas SJ et al. Modeling of surface roughness in precision machining of metal matrix composite using ANN. J Mater Process: Technol. 2008;197:439-444. https://doi.org/10.1016/j.jmatprotec.2007.04.121
2. Das MK, Kumar K, Barman TK et al. Optimization of Surface Roughness and MRR in Electrochemical Machining of EN31 Tool Steel using Grey-Taguchi Approach. Proceed Mat Sci. 2014;6:729-740. https://doi.org/10.1016/j.mspro.2014.07.089.
3. Wang J, Bai X, Shen X et al. Effect of micro-texture on substrate surface on adhesion performance of electroless Ni-P coating. J Manuf Proc. 2022;74:296307. https://doi.org/10.1016/j.jmapro.2021.12.025.
4. Agarwala RC, Agarwala V. Electroless alloy composite coatings: A review. Sadhana - Acad Proceed Eng Sci. 2003;28:475-93. https://doi.org/10.1007/BF02706445

5. Davoodi D, Emami AH, Vaghefi SMM et al. Deposition of electroless Ni-Cu-P coatings on L80 steel substrates and the effects of coatings thickness and heat treatment on the corrosion resistance. Int J Press Vesselsand Pip. 2022;200:104823. https://doi.org/10.1016/j.ijpvp.2022.104823

6. Valova E, Armyanov S, Franque A et al. Electroless deposited Ni-Re-P, Ni-W-P and Ni-Re-W-P alloys. J Appl Electrochem. 2001;31:1367-1372. https://doi.org/ 10.1023/A:1013862729960

7. Ren L, Cheng Y, Han Z et al. Investigation on the mechanical performance of the electroless Ni-W-P coating based on fractal theory. Surf Topog: Metrolog Propert. 2019;7:025017. https://doi.org/10.1088/2051-672X/ab2038

8. Liu Y, Zhao Q. Study of electroless Ni-Cu–P coatings and their anti-corrosion properties. Appl Surf Sci. 2004;228:57-62. https://doi.org/10.1016/j.apsusc.2003.12.031

9. Shu X, Wang Y, Lu X et al. Parameter optimization for electroless Ni-W–P coating. Surf Coat Technol. 2015;276:195-201. https://doi.org/10.1016/j.surfcoat.2015.06.068

10. Balaraju JN, Rajam KS. Electroless deposition of Ni-Cu-P, Ni-W-P and Ni-W-Cu-P alloys. Surf Coat Technol. 2005;195:154-161. https://doi.org/10.1016/j.surfcoat.2004.07.068

11. Li J, Wang D, Cai H et al. Competitive deposition of electroless Ni-W-P coatings on mild steel via a dual-complexant plating bath composed of sodium citrate and lactic acid. Surf Coat Technol. 2015;279:9-15. https://doi.org/10.1016/j.surfcoat.2015.08.017

12. Yu J, Zhai S, Yu M et al. Effects of Sodium Hypophosphite on the Behaviors of Electrodeposited Ni-W-P Alloy Coatings. J Mat Eng Perf. 2017;26:3915. https://doi.org/10.1007/s11665-017-2807-3

13. Duari S, Mukhopadhyay A, Barman TK et al. Study of wear and friction of chemically deposited Ni-P-W coating under dry and lubricated condition. Surf Interfa. 2017;6:177-189. https://doi.org/10.1016/j.surfin.2017.01.009

14. Oliveira MCL, Correa OV, Ett B et al. Influence of the Tungsten Content on Surface Properties of Electroless Ni-W-P Coatings. Mat Res. 2017;21:0567. https://doi.org/10.1590/1980-5373-MR-2017-0567

15. Elansezhian R, Ramamoorthy B, Nair PK. Effect of surfactants on the mechanical properties of electroless (Ni-P) coating. Surf Coat Technol. 2008;203:709-712. https://doi.org/10.1016/j.surfcoat.2008.08.021

16. Ariffah MSN, Nurulakmal MS, Anasyida AS et al. Surface roughness, wear and thermal conductivity of ternary electroless Ni-Ag-P coating on copper substrate. Mat Res Express. 2020;7:026536. https://doi.org/10.1088/2053-1591/ab71c4

17. Wu FB, Tiena SK, Duha JG et al. Surface characteristics of electroless and sputtered Ni-P-W alloy Coatings. Surf Coat Technol. 2003;166:60-66. https://doi.org/10.1016/S0257-8972(02)00725-9

18. Novakovic J, Vassiliou P, Samara KI et al. Electroless NiP-TiO$_2$ composite coating, their production and properties. Surf Coat Technol. 2006;201:895-901. https://doi.org/10.1016/j.surfcoat.2006.01.005

19. Yanhai C, Shuai C, Qingqiang H et al. Effect of Tungsten Addition on the Anti-fouling Property of the Electroless Ni-W-P Deposits. Rare Metal Mat Eng. 2016;45:1931-1937. https://doi.org/10.1016/S1875-5372(16)30149-7

20. Behrens A, Ginzel J. Neuro-fuzzy process control system for sinking EDM. J Manuf Proc. 2003;5:33-39. https://doi.org/10.1016/S1526-6125(03)70038-3

21. Vinayagamoorthy R, Manoj I, Kumar GN et al. A central composite design based fuzzy logic for optimization of drilling parameters on natural fiber reinforced composite. J Mech Sci Technol. 2018;32:2011-2020. https://doi.org/10.1007/s12206-018-0409-0

22. Vijayanand M, Varahamoorthi R, Kumaradhas P. Artificial neural network modelling for average surface roughness in citrate stabilised electroless nickel boron coatings. Mat Today: Proceeds. 2022;49:2239-2244. https://doi.org/10.1016/j.matpr.2021.09.335

23. Pedrycz W. Fuzzy equalization in the construction of fuzzy sets. Fuzzy Sets Syst. 2001;119:329-335. https://doi.org/10.1016/S0165-0114(99)00135-9

24. Kar S, Chakraborty S, Dey V et al. Optimization of Surface Roughness Parameters of Al-6351 Alloy in EDC Process: A Taguchi Coupled Fuzzy Logic Approach. J Instit Eng (India): Ser C. 2017;98:607-618. https://doi.org/10.1007/s40032-016-0297-y

25. Das B, Roy S, Rai RN et al. Surface roughness of Al-5Cu alloy using a Taguchi-fuzzy based approach. J Eng Sci Technol Rev. 2014;7:217-222. https://doi.org/10.25103/jestr.072.32

26. Kao CC, Albert JS, Miller SF. Fuzzy logic control of Microhole electrical discharge machining. J Manuf Sci Eng. 2008;130:1-6. https://doi.org/10.1115/1.2977827

27. Venkatesha C, Arunb NM, Venkatesan R. Optimization of micro drilling parameters of B4C DRMM Al 6063 composite in µECM using Taguchi coupled fuzzy logic. Proced Eng. 2014:97:975-985. https://doi.org/10.1016/j.proeng.2014.12.374.

28 Aamir M, Tu MS, Rad MT et al. Optimization and Modelling of Process Parameters in Multi-Hole Simultaneous Drilling Using Taguchi Method and Fuzzy Logic Approach. Materials. 2020;13:680. https://doi.org/10.3390/ma13030680

29. Sarkar S, Baranwal RK, Lamichaney S et al. Optimization of electroless Ni-Co-P coating with hardness as response parameter: A computational approach. J Tribologi. 2018;18:81-96.